Chapter 2

Semiconductor Surfaces and Interfaces

The experiments that we will focus on here are using nanoscale devices formed in 2D electron gases in GaAs/AlGaAs heterostructures, consisting of several layers that are brought into contact at interfaces. Surfaces and interfaces therefore play a very important role and are the topic of this chapter.

At the surface of a semiconductor crystal to vacuum, the bands of the solid get related to the vacuum energy level. It takes a finite amount of energy to remove electrons from the crystal to the vacuum, since formation of the crystal from far separated atoms lowered the energy. The *work function* Φ_A is the energy to transfer one electron at the chemical potential from the crystal into the vacuum. In pure semiconductors and in insulators, there are no states at the chemical potential. Hence, the *electron affinity* is introduced as the energy difference from the bottom of the conduction band to the vacuum energy level. Both the affinity and the work function are dependent on the bulk crystal/material properties.

2.1 Electronic Surface States

The periodic pattern of chemical bonds in the crystal is interrupted at the surface, resulting in unsaturated (dangling) bonds, which can rearrange themselves (surface reconstruction) and/or which might be saturated by a (mono)layer of adatoms (sometimes oxygen). This results in a change of both the surface crystal structure and the allowed energies that depend sensitively on the materials and bulk crystal structures involved. Often, the electronic surface structure has little to do with the bulk structure. The surface states can be probed, for example with scanning tunneling techniques or with photo emission spectroscopy. For simplicity, we consider here the case without surface reconstruction and without passivation, assuming essentially the perfect periodic crystal is simply cut off in a plane. This will give a qualitatively correct picture.

While not giving a derivation here, a simple motivation for formation of electronic surface states goes as follows: Bloch's theorem in principle allows the wave vector in the wave function $\psi_k(r) = e^{ik \cdot r} u_k(r)$ to be a complex number. An imaginary wave vector corresponds to an exponentially damped wave function, an "evanescent wave". In an infinite,

perfect crystal, that is not physical, since it would specify a special location in the crystal, violating periodicity or translational symmetry. But the surface breaks translational symmetry, therefore allowing wave vectors with nonzero imaginary component. It can be shown that the resulting states are localized at the surface, with a wave function amplitude that decays exponentially over a few lattice constants when going from the surface into the bulk. It turns out that the energies of these states are usually located inside the band gap, forming a separate band of surface states (see figure 2.1) that coexists at the surface with the usual semiconductor conduction and valence bands.
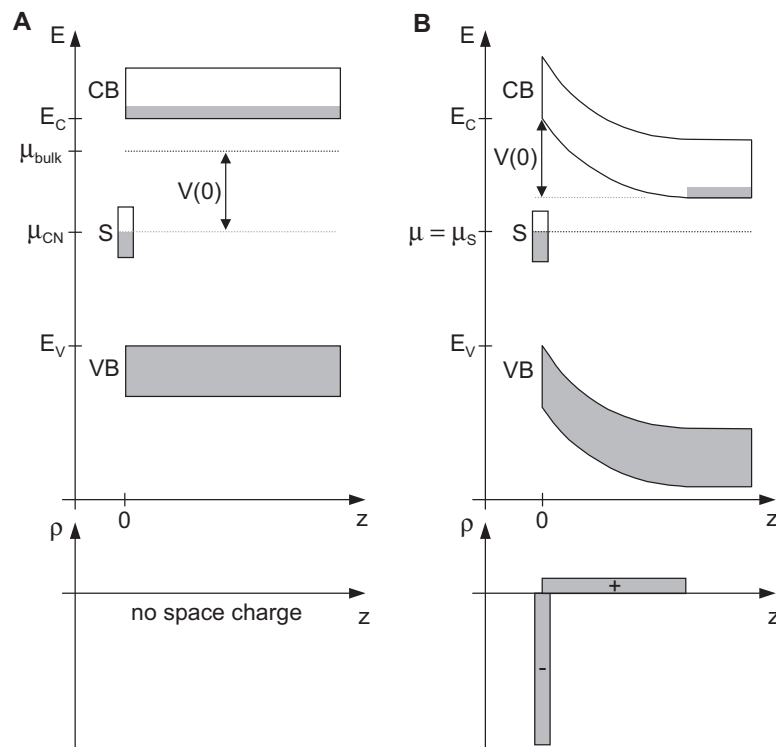

Figure 2.1: Band structure at the surface of an n-doped semiconductor before (**A**, left) and after (**B**, right) equilibration. Gray indicates occupied states. To match chemical potentials at the surface and in the bulk, charge builds up on the surface depleting the donor charges a depth into the bulk and bending the bands accordingly.

The number of surface states per area is essentially given by the number of atoms per area at the surface. These states can be comprised of states that in the infinite, boundary less crystal would have contributed to either the conduction or the valence bands and can be an admixture of both types of bands. Due to charge neutrality, in the case of the intrinsic semiconductor the number of filled surface states is equal to the number of electrons that were removed from the bulk valence band due to surface formation, resulting in a neutral, uncharged surface. The remaining surface states are empty. Filled surface states have electrons that in principle could be given into empty available states and can therefore be considered donor-like states. Vice-versa: empty surface band states are called acceptor-like. The energy up to which the surface states (within the surface band) are filled in the intrinsic, un-doped semiconductor is dictated by charge neutrality and is sometimes referred to as the charge neutrality level or *charge neutrality chemical potential* μ_{CN}.

2.2   The Semiconductor-Vacuum interface

For a surface of a doped semiconductor, electrons occupying the conduction band (originating from the dopants) can lower their energy by filling empty surface band states (if available, which is often the case). This gives a net surface charge n_S (charge per area, in this case negative) which is balanced to maintain charge neutrality by a region inside the crystal of equal total charge of opposite sign (positive)—referred to as *depletion region*. The charge in the depletion region is due to holes left behind from conduction band electrons that dropped into the surface band. The surface charge n_S is located within a few lattice constants around the surface, forming a 2D electron gas. The dopant density is to some extent arbitrary and can be externally controlled. It is often chosen by various other considerations, see the heterostructure section, usually resulting in a dopant density that is much lower than the available surface states, typically of the order of one dopant atom for every 10'000 crystal atoms. Therefore, this results a depletion region that can reach many lattice constants into the bulk.

2.2.1   Band bending

For a bit more quantitative consideration, let z_{dep} denote the extent of the depletion region into the bulk starting from the surface at $z = 0$ (see figure 2.1) and N_D the dopant density (per m^3). All donors are ionized in the depletion region giving a space charge density of $\rho = eN_D$. The Poisson equation for the z-dependence of the potential $V(z)$ within the depletion region $0 \leq z \leq z_{dep}$ is

$$\frac{d^2V}{dz^2} = -\frac{e^2 N_D}{\epsilon\epsilon_0} \quad \Rightarrow \quad V(z) = -\frac{e^2 N_D}{2\epsilon\epsilon_0}(z - z_{dep})^2, \tag{2.1}$$

where the normalization of V was chosen as $V = 0$ in the bulk (for $z > z_{dep}$) and the constant of integration was chosen to match $V(z_{dep}) = 0$ accordingly. According to Eq. 2.1, the bands are therefore *bending* quadratically, with a total shift of $V(z \to 0^+) = -e^2 N_D z_{dep}^2/(2\epsilon\epsilon_0)$. More generally, the local curvature of a band is proportional to the local space charge density, according to Eq. 2.1. At the surface $z = 0$, V(z) will jump (over the narrow extent of the surface charge accumulation layer), due to the charge n_S accumulated strongly localized at the surface. This is not indicated in figure 2.1 since it is very narrow compared to the depth z_{dep} of the depletion region. The surface accumulation charge is of equal size but opposite sign as the total depletion region charge: $n_S = -N_D z_{dep}$ (charge neutrality) and creates a further change in V that we neglect. In this approximation, the bands have bent by a total amount of $\Delta V = V(0)$.

At the surface, the chemical potential is in the surface band (since that band is partly filled for sufficiently low doping density), and the surface band energy and width depends on material properties. In the bulk, the chemical potential is in the gap, usually closer to the conduction band (again, depending of the doping density). However, in equilibrium, the chemical potential has to be the same everywhere, and in particular needs to be the same at the surface and in the bulk. This condition therefore dictates the value of ΔV, i.e. the amount by which the bands need to bend, originating from the material dependent surface properties, and therefore determines the depletion depth z_{dep}.

2.2.2 Fermi Level pinning

To make an example, let's assume that the surface band is centered in the middle of the gap, with a width of a fraction of the gap size, and is half filled in the intrinsic material. Doping will fill the surface band slightly more. Let's take the case of $GaAs$ with gap $E_g = 1.4 \, \text{eV}$, a typical doping of $N_D = 10^{24} m^{-3}$ (corresponding to about 1 dopant for every 10^4 crystal atoms, or about 1 dopant for every 20 atoms along a crystal axis). Then, $\Delta V \sim E_g/2$, and with $\epsilon \sim 13$ and using

$$z_{dep} = \sqrt{\frac{2\epsilon\epsilon_0 \Delta V}{e^2 N_D}} \tag{2.2}$$

it follows that $z_{dep} \sim 30\,\text{nm}$, or about 60 lattice constants. This results in a surface charge of $n_S = z_{dep} N_D \sim 3 \times 10^{16} m^{-2}$, much smaller than the total surface density of states $\sim 2/a_0^2 \sim 6 \times 10^{18} m^{-3}$, with lattice constant $a_0 \sim 5.5 \text{Å}$. Therefore, the chemical potential μ_S at the surface is essentially independent of the doping level (at least for typical doping densities as above). One says that the Fermi level is *pinned* at the surface. Particularly considering that the surface atoms make up a very small fraction of the total number of atoms in the crystal, the role of the surface is quite important. Also, note that the depletion depth z_{dep} can be changed with the dopant density as formulated in Eq. 2.2.

2.3 Metal-Semiconductor Interface: Schottky Barrier

One important type of interface is the one between a metal and a semiconductor. Among various possible scenarios depending on the respective alignment of the bands and chemical potentials, two important cases are the *Schottky barrier* and *Ohmic contacts*. If a Schottky barrier forms, charge can move from the metal into the semiconductor only by tunneling through a barrier; we first discuss this situation. The most relevant case is the situation when the chemical potential in the conduction band of the metal lies inside the gap of the semiconductor. At the interface, it can be shown that presence of the metal creates *induced gap states* (IGS) within the gap of the semiconductor, as shown in figure 2.2A, displaying the interface before before charge transfer occurred.

Let's start with this situation and let's further assume an intrinsic (undoped) semiconductor. The common energy scale is clearly the vacuum energy level. In general, the chemical potential in the metal μ_M is not aligned with either the surface chemical potential μ_S nor the bulk semiconductor chemical potential μ_{SC}, but often one finds $\mu_M \geq \mu_S$. Now we allow charge transfer. Electrons from the metal can lower their energy by filling empty surface states, thereby leaving behind holes in the metal. A charge dipole located at the interface results and aligns μ_M and μ_S, via the dipole potential obeying the Poisson equation, similar to Eq. 2.1, and corresponding band bending in the semiconductor by an amount $\Delta\mu = \mu_M - \mu_S$. This dipole and band bending is strongly localized at the surface since the surface states decay exponentially over a few lattice constants into the bulk semiconductor. The chemical potential μ_M of the metal is essentially unchanged, since the number of available electrons in the bulk metal is very large compared to the necessary number of electrons to fill the surface states up to μ_M. The resulting situation is depicted in figure 2.2B.

To transfer electrons from the metal into the *bulk* semiconductor, a barrier of energy (see figure 2.2) $V_S = \Phi_M - \chi_e + \Delta\mu$—the Schottky barrier—has to be overcome, which
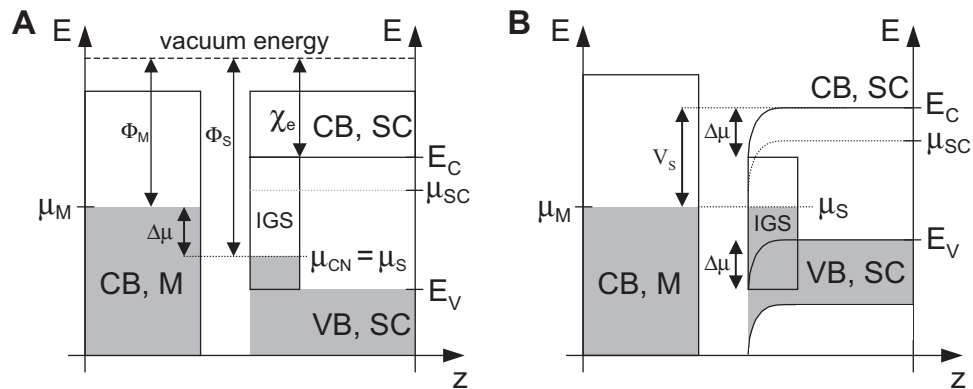
Figure 2.2: Band structure of a metal-semiconductor interface before (left, A) and after (partial) charge transfer (right, B). Shown here is case where the chemical potential of the metal is situated inside the semiconductor gap, which results in a Schottky barrier V_S increased by $\Delta\mu = \mu_M - \mu_S$ due to surface charge accumulation when the bands bend to match $\mu_M = \mu_S$. IGS denotes induced gap states. For an intrinsic semiconductor, $\mu_{SC} = \mu_S$, and B represents thermodynamic equilibrium. For the doped semiconductor $\mu_{SC} \neq \mu_S$ and further charge is transferred, as detailed in Figure 2.3.

just became larger by $\Delta\mu$ due to the surface charge accumulation. In an intrinsic semiconductor, the entire system is then in a thermodynamic equilibrium, since in the intrinsic case $\mu_{SC} = \mu_S$. In a doped semiconductor, however, there is still a missmatch $\mu_S \neq \mu_{SC}$. By a further charge transfer of donor electrons onto the surface and corresponding band bending, $\mu_S = \mu_{SC}$ will be achieved, directly analogous to the situation described before for the semiconductor-vacuum interface, resulting in the band diagram in figure 2.3.
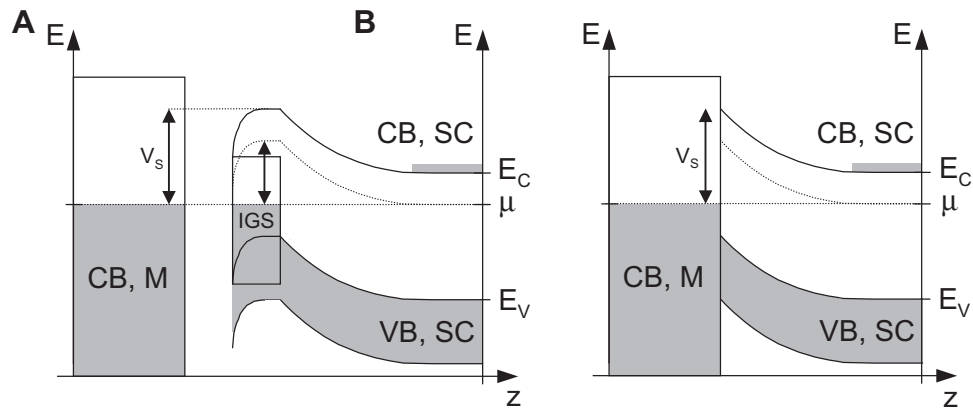

Figure 2.3: Band structure of a metal-semiconductor interface where the semiconductor is doped and the system in in thermodynamic equilibrium (left, A). The right panel shows a simplified view omitting the semiconductor surface. V_S denotes the Schottky barrier.

2.3.1   Schottky model

As derived the expression for the Schottky barrier $V_S = \Phi_M - \chi_e + \Delta\mu$ depends on the (often complicated and difficult to calculate) surface properties via the surface chemical potential μ_S in $\Delta\mu = \mu_M - \mu_S$, while the metal work function Φ_M and the electron affinity in the semiconductor χ_e are bulk parameters. The Schottky model neglects the surface effects and takes $V_S = \Phi_M - \chi_e$. This is equivalent to arguing that removing electrons with

affinity χ_e from the semiconductor and adding them to the metal with work function Φ_M will lead to a depletion region in the semiconductor establishing equilibrium and forming a barrier of height $V_S = \Phi_M - \chi_e$. A corresponding band diagram is shown in Figure 2.4 together with some measured barrier heights for metals on GaAs and Si.
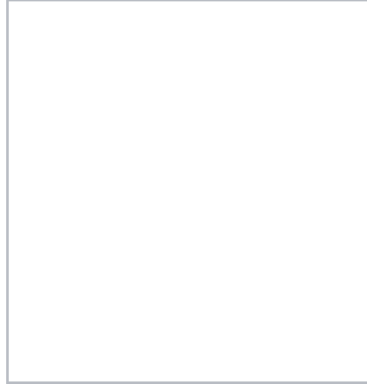
Figure 2.4: (left) Band diagram in the Schottky model. (right) Schottky barrier height of Si and GaAs in contact with different metals as a function of the metal work function. From Sze, 1985.

2.3.2   Schottky diode

The metal-semiconductor interface with a Schottky barrier acts as a diode, the Schottky diode, which has been discussed at length in the literature. Suffice it here to state that conduction through this diode depends on the tunneling current through the barrier, which varies exponentially with barrier width and height. Applying a voltage V to the metal with respect to the grounded semiconductor changes the chemical potential of the metal and therefore can be used to control the barrier, resulting in an the exponential I-V curve of a diode. A positive Voltage will reduce the barrier height (and therefore also the barrier width) via $V_S = \Phi_M - eV - \chi_e$. When a Voltage of $V \sim V_S$ is applied, large currents will flow. Typical Schottky barrier heights for metals on GaAs are about $0.8\,\mathrm{eV}$. On the other hand, the currents can be extremely small for negative voltages, corresponding to the diodes reverse bias direction, and the resulting current is called *leakage current*.
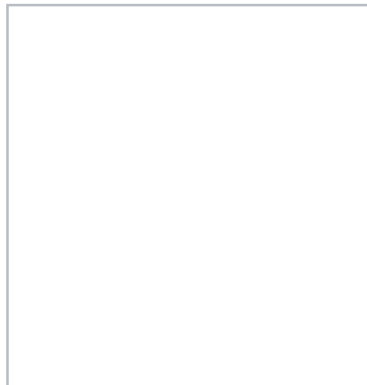
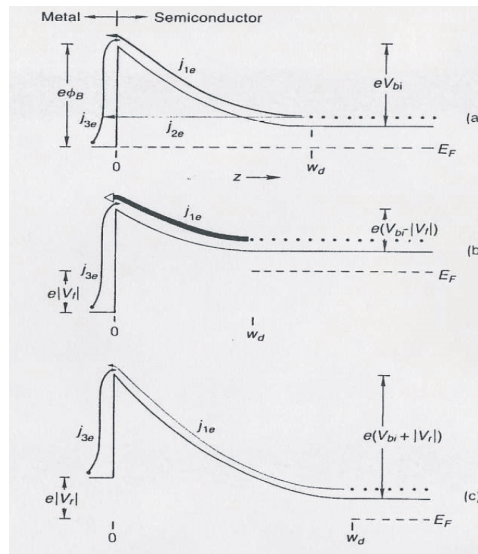Figure 2.5: I-V characteristic of the Schottky diode. (from Heinzel)

Figure 2.6: left: Schottky barriers under a) no bias, b) forward bias ($V > 0$) and c) reverse bias ($V < 0$). Also indicated are various electron currents components in a Schottky barrier: j_{1e} and j_{3e} are injection currents, which are thermally driven/excited, j_{2e} is the tunneling current. At low temperatures, the termionic currents can be neglected. [Look 1988]

2.4   GaAs Heterostructures and 2D electron gas

- To determine the band structure of the heterostructure, a self consistent solution of Poisson and Schrödinger equation has to be found, usually numerically and iteratively

- A triangular quantum well forms at the $AlGaAs/GaAs$ interface, referred to as the *heterointerface*. Often, only the quantum mechanical ground state in the triangular well is populated (at low temperatures, $T \lesssim 100K$), making this one of the best experimental realizations of a 2D system in nature that we know. This 2D electron gas s often abbreviated 2DEG. Typical widths of the wave function are about 10 nm, which means there are still some observable finite size effects, particularly in large magnetic fields. It is also possible to grow another $AlGaAs$ layer below the heterointerface shown here, resulting in a square well.

- Two structures can be distinguished: one where doping over an extended z region is used, see Figure 2.8, left. The other where the doping is localized in just a few atomic layers, called δ-*doping*, see Figure 2.8, right.

- As long as the dopants are removed from the lower $GaAs/AlGaAs$ interface, it is referred to as *modulation doping*, a technique first demonstrated by Dingle in 1978.

- Choosing the right Si-doping density is an issue of fine-tuning and very sensitive. Possible problems: parallel conduction (in the dopant layer), second subband population, no electrons in well, too high or too low carrier density in well.

- Typical Al concentration is $x \sim 0.3$, putting the conduction band of $Al_{0.3}Ga_{0.7}As$ about 300 meV above the conduction band of $GaAs$ and the top of the $Al_{0.3}Ga_{0.7}As$ valence band 160 meV below the $GaAs$ valence band.

- Usually, Si is used as the dopant. It only goes into the doping region (either into the δ layer or into a larger width band within the $AlGaAs$), all the other regions are intrinsic semiconductors

- Only a fraction of the donor atoms are ionized. Part of that fraction goes into surface states, and part into the quantum/triangular well
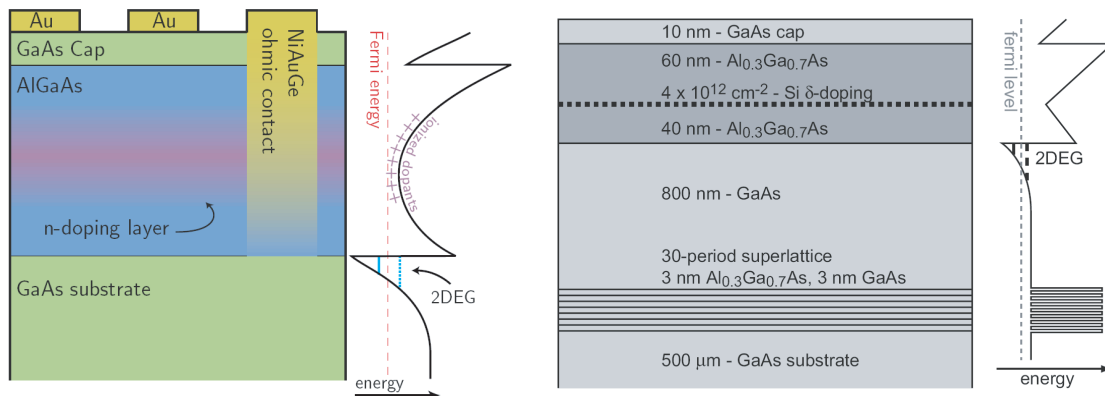

Figure 2.7: Growth profile and bandstructure of typical GaAs heterostructures.

- Two charge dipoles build up: one between surface and doping layers, and one between heterointerface and dopant layer, both resulting in electric fields between the respective layers, giving a finite but constant slope to the bands between dipoles in regions without extra charge.

- The last $GaAs$ layer making interface with vacuum is called *cap layer* and prevents oxidation that would occur was the $AlGaAs$ layer exposed to air/oxygen.

- Very large mobilities reaching $\sim 33 \times 10^6 cm^2/(Vs)$ corresponding to a mean free backscattering path of about $\sim 300\,\mu$m have been achieved.
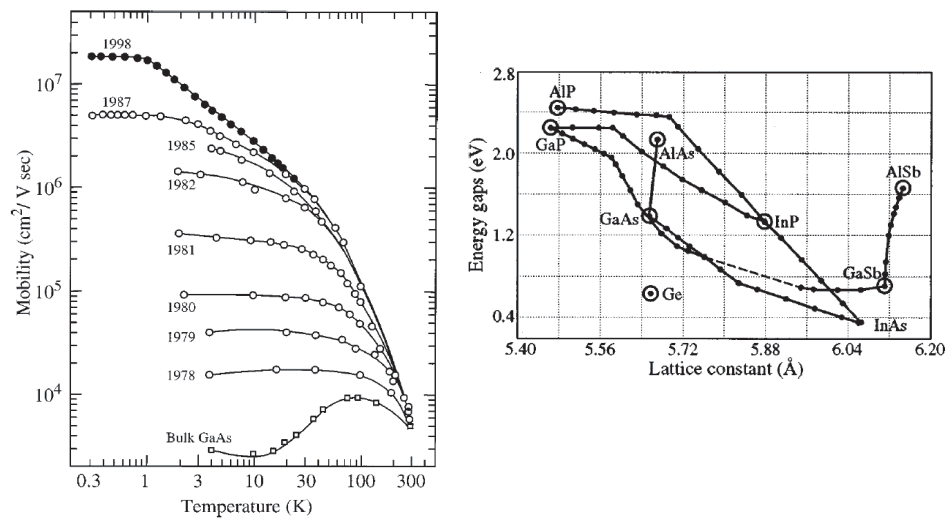

Figure 2.8: left: progress made over the years in mobility μ of electrons in a 2DEG in modulation doped GaAs/AlGaAs as a function of temperature. At high temperatures, μ is limited by scattering with phonons of the bulk. At the lowest temperatures, μ is limited by impurities and defects. [Stormer 1989] right: energy gaps as a function of the lattice constant for III-V semiconductors. [Alferov 2001]

- These very large mobilities/clean samples/long mean free paths are possible because:

   1. the heterointerface quality is excellent, not disrupting the crystal periodicity across the interface, with lattice constants of $AlGaAs$ and $GaAs$ matched within 0.5% ($AlGaAs$ condenses also into a Zinc-blende crystal). This is in stark contrast to the Si/SiO_2 interface, where the SiO_2 condenses into a highly disordered, glassy phase that is not at all matching the Si crystal, which results in severe interface scattering, reducing mobility of electrons.

   2. the ionized donors—a significant source of scattering—are spatially well separated from the 2DEG, usually between $20\,$nm $- 120\,$nm. Consequently, the screened Coulomb potentials the electrons see are much weaker and create predominantly small angle scattering, not very efficient at backscattering (full $180°$ scattering).

- By controlling the Al content the z-dependence of the band gap/band structure can be custom engineered, if desired. For example, quantum wells can be grown with a Al content quadratic in z, going from, say, 30% Al content to zero back to 30%, a so called *parabolic* well, resulting in a harmonic oscillator in the z-direction. By

top and bottom gating, the center of mass/maximum of the wave function can be shifted in the z-direction, changing the average Al content the electrons feel. Because the Lande g-factor depends on the Al concentration (it can even change sign), the g-factor can be controlled with a gate. Basically any desired potential can be grown in this way.

- By shining light on the waver, additional donors can be ionized, giving an increased density and also increased mobility, which persists over long periods of time while the sample is kept cold ($\lesssim 50\,\mathrm{K}$), often referred to as *persistent photoconductivity*.

2.5   Screening

Conduction electrons populate all states up to the Fermi energy, but the bottom of the potential is varying in a disordered manner, due to the Coulomb potentials of the ionized donor atoms and other defects and impurities. These potentials create a complicated potential mountain-valley landscape. In high mobility samples, most maxima lie below the Fermi energy, screening is efficient, and only a sparse few peaks reaching above E_F. If the density in the 2DEG is lowered, say with a top gate, then the Fermi energy correspondingly is reduced, and more peaks may appear piercing the Fermi level, giving more backscattering and a reduction in mobility. (Sometimes the analogy to the "Bath-tub potential" is made, where the water represents the electrons.)

A detailed theory of screening is left to the proper condensed matter theory lecture. Here, it be mentioned that screening can be expressed by a dielectric function $\epsilon(\omega, \vec{q})$. In Thomas-Fermi approximation, a screening length scale appears, the *Thomas-Fermi screening length*, which is usually of the order of the Fermi-wavelength. An external potential (here a Coulomb scatterer) in 3D

$$V_{ext}(r) = \frac{-Ze}{r} = \frac{-Ze^2}{(2\pi)^3} \int \frac{4\pi}{q^2} e^{\imath \vec{q}\vec{r}} d\vec{q} \tag{2.3}$$

will be screened to an effective potential electrons in the semiconductor will see:

$$V_{eff}(\vec{q}) = \frac{V_{ext}(\vec{q})}{\epsilon(\vec{q})}, \quad V_{eff}(r) = \frac{-Ze^2}{(2\pi)^3} \int \frac{1}{\epsilon(\vec{q})} \frac{4\pi}{q^2} e^{\imath \vec{q}\vec{r}} d\vec{q} \tag{2.4}$$

via a induced charge density variation that can be calculated to be:

$$\rho_{ind}(\vec{r}) = \frac{Ze}{\pi} \frac{k_{TF}^2}{k_F^2(4 + k_{TF}^2/2k_F^2)} \frac{\cos(2k_F r)}{r^3} \tag{2.5}$$

This charge density is periodically modulated with a period of half the fermi wavelength (known as *Friedel oscillations*) and decays as r^{-3} in distance (in 3D) from the scatterer. This can be understood in terms of a standing wave due to a superposition of the incoming and from the scatterer reflected waves. This is a result that depends on the dimensionality considered, indeed in 2D, as applicable for a 2DEG, one obtains:

$$V_{eff}(\vec{r}) = \frac{Ze}{\epsilon\epsilon_0} \frac{4k_T F k_F^2}{(2k_F + k_{TF})^2} \frac{\sin(2k_F r)}{2k_F r^2} \tag{2.6}$$

where the oscillations now have a longer range, decaying only as r^{-2}.

2.6   Scattering GaAs

2.6.1   Bulk GaAs scattering

Various scattering mechanisms contribute, which according to the Mathiesen rule can be added up as scattering rates to give the total scattering rate: $1/\mu = \sum_i 1/\mu_i$. Here, some scattering types are listed, first discussed for the bulk 3D GaAs case:

- impurity scattering: *neutral impurities* usually give very small scattering cross sections. Charged or *ionized impurities* represent (screened) Coulomb scatterers with peak potentials that can be comparable to the Fermi energy. At higher temperatures, electrons have larger kinetic energy and will be deflected by a smaller angle, giving larger mobility at higher temperatures. Calculations give a temperature dependence of the mobility $\propto T^{3/2}\log(T)$ in 3D.

- electron-phonon (lattice vibrations) scattering: the only scattering mechanism in perfect, pure crystals.

- electron-phonon scattering, *deformation potential*: scattering at the lattice deformation caused by phonons. Acoustic phonons are usually most relevant, which can be treated as quasi-elastic since the energy transfers are small. The temperature dependence of the corresponding mobility (scattering rate) is given by $n_{ac}/\overline{v}$, where n_{ac} is the density of acoustic phonons and $\overline{v}$ is the average electron velocity. n_{ac} is proportional to the Bose-Einstein distribution, scaling as $1/T$ at for temperatures large compared to the phonon energy and $\overline{v} \propto \sqrt{T}$, giving a mobility contribution $\propto T^{-3/2}$.

- electron-phonon scattering, *polar scattering*: *GaAs* is a polar crystal, lattice vibrations are accompanied by oscillating electric fields, particularly strong for optical phonons. For $kT \gg \hbar\omega_{op}$ where $\omega_{op} \sim 5\,\mathrm{meV}$ denotes the optical phonon energy, the resulting mobility varies as $T^{-1/2}$

- electron-phonon scattering, *piezo-electric scattering*: *GaAs* is also piezoelectric, meaning that a polarization field develops in response to a crystal deformation, also with a $T^{-1/2}$ contribution.
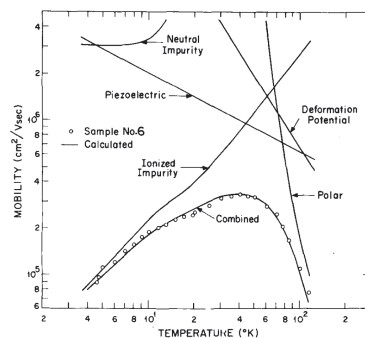

Figure 2.9: Various scattering mechanisms in bulk showing measured (circles) and calculated (curves) mobilities as a function of temperature. The bulk sample had a donor density $n_D = 4.8 \times 10^{19}\,\mathrm{m}^{-3}$ and an acceptor density $n_A = 2.1 \times 10^{10}\,\mathrm{m}^{-3}$ [Stillman 1976].

2.6.2   GaAs 2DEG scattering

Scattering in a 2D electron gas is different from the bulk case because the screening and phase space properties of the electrons are now 2D, while the scattering potentials are still three-dimensional. Decay of the Friedel oscillations in 2D is weaker than in 3D, as mentioned before. Also, new scattering mechanisms arise due to the interface and remote impurities. Relevant mechanisms include:
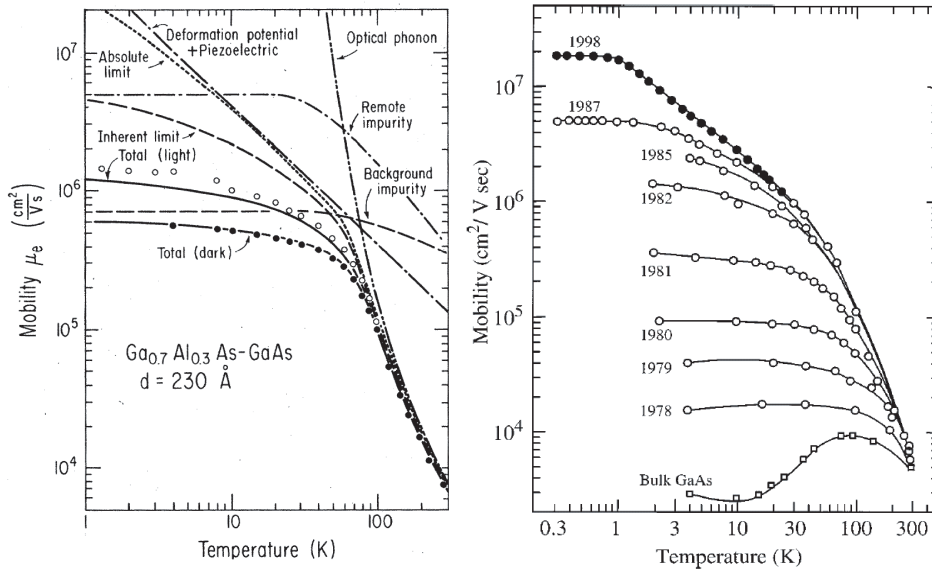

Figure 2.10: Various scattering mechanisms in a *GaAs* 2DEG showing measured (circles) and calculated (curves) mobilities as a function of temperature. The used 2DEG had was measured both in the dark (open circles, $n = 2.2 \times 10^{11} \, \mathrm{cm}^{-2}$) and after illumination (filled circles, $n = 3.8 \times 10^{11} \, \mathrm{cm}^{-2}$), with a spacer thickness $d = 23 \, \mathrm{nm}$ and a modulation doping density of $8.6 \times 10^{22} \, \mathrm{m}^{-3}$ distributed evenly within a $20 \, \mathrm{nm}$ layer between spacer and surface. A homogeneous density of backgroun impurities of $9 \times 10^{19} \, \mathrm{m}^{-3}$ was assumed, a typical number for high quality bulk *GaAs*. [Walukiewicz, 1984]

- *impurities* divided into *remote, ionized donors* that are now spatially separated from the 2DEG by a spacer layer. A small *residual donor density* remains inside the electron gas (and everywhere in the crystal), and can be improved by simply obtaining cleaner materials. Both of these mechanisms can be quite important. Intuitively, one would guess that the farther away the donors are, the lower the scattering they induce is. That is correct, but as the donor layer is further removed from the heteroinferface, the density and thereby mobility in the 2DEG is reduced, unless other parameters are also changed, making further separation of donors from the interface a complicated undertaking.

- *interface roughness* interface imperfections and roughness represents deviation from the perfect crystal and can therefore create scattering. Due to crystal matching, in *GaAs/AlGaAs* heterostructures this type of scattering is usually very small, unlike the case of the $Si - MOSFET$.

- *alloy scattering* In $Al_xGa_{1-x}As$, 30% of the Ga atoms are replaced by Al, but this occurs in a random, disordered fashion, resulting in a non-periodic potential. For *GaAs* 2DEG's, the electron wave function almost entirely resides in the crystalline

GaAs and only an exponentially small tail protrudes into the *AlGaAs*, making alloy scattering also irrelevant.

- *inherent limit* the mobility that would result in a sample without the background impurities but including the remote donors

2.7   Ohmic Contacts

Despite 40 years of electrical measurements in *GaAs* and 20 years of 2DEG experiments, making contacts is still not always trivial and the the exact contact mechanism is not completely understood. There are standard recipes that usually work, but depending on the exact structure and application some modifications or fine tuning is often necessary. We define a good ohmic contact to be a source of carriers with a non-zero internal resistance R_c which obeys Ohm's law for all current densities of interest. As discussed previously, a metal on the surface of a *GaAs/AlGaAs* results normally in a Schottky barrier behaving as a diode, highly non-linear, and certainly not suited as an Ohmic contact. The contact needs to work at the lowest temperatures reached in experiments. In this regime, thermionic currents are negligible, but tunnel currents remain a possibility.

The probability of an electron to tunnel from the semiconductor into the metal depends exponentially on height V_{bi} and width w_d of the barrier and can be estimated in WKB approximation:

$$T(w_d) = \exp\left[-2\int_{w_d}^0 \left\{\frac{2m^*}{\hbar^2}V(z)\right\}^{1/2} dz\right], \qquad (2.7)$$

where $V(z)$ describes the shape of the barrier, with $V(w_d) = 0$. Solving the Poisson equation, we previously found a quadratic dependence on z, see Equation 2.1, which we substitute here into the integral. Further, we determined the width of the barrier, Eq. 2.2. Here we use $\Delta V = e(V - V_{bi})$, with V_{bi} the bias independent barrier height and V an external applied Voltage. The integral is then trivial to compute:

$$T = \exp\frac{e(V - V_{bi})}{\mathcal{E}_0}, \qquad (2.8)$$

where we introduced the energy

$$\mathcal{E}_0 = \frac{\hbar}{2}\left(\frac{e^2 N}{\epsilon\epsilon_0 m^*}\right)^{1/2} \qquad (2.9)$$

characterizing the barrier. $\mathcal{E}_0$ depends on the doping density, and for an achievable doping density $N \sim 10^{25} m^{-3}$ one obtains $\mathcal{E}_0 \sim 60\,\text{meV} \sim 700\,\text{K} \times k$. As before, large doping gives small barrier diameter. The tunneling current density j is then

$$j \propto \left\{1 - \exp\left(\frac{eV}{\mathcal{E}_0}\right)\right\} \approx \frac{eV}{\mathcal{E}_0} + O(V^2) \qquad (2.10)$$

where the expansion of the exponent is valid for small Voltages $eV \ll \mathcal{E}_0$. We therefore find ohmic behavior in the small bias range. The factor $\exp(-eV_{bi}/\mathcal{E}_0)$ still multiplies the entire expression, suppressing the current. Unfortunately, the barrier height cannot be made smaller by a proper choice of metal (surface state density is large). Further, this
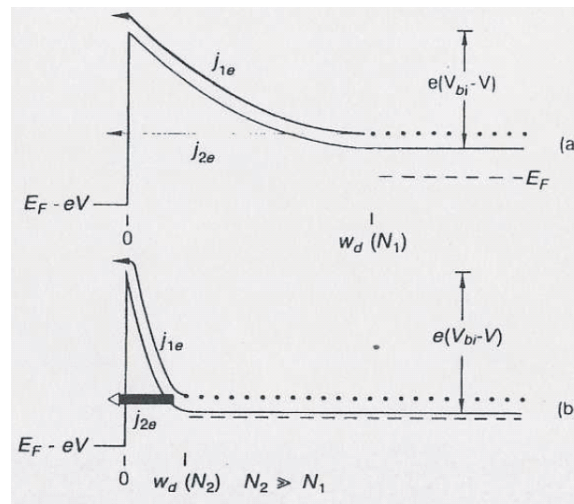
Figure 2.11: upper: doping density N_1, lower: much higher doping $N_2 \gg N_1$. The reduction of the depletion width w_d and consequent increase of the electron tunneling current j_{2e}. [Look 1988]

simple model cannot explain experimentally fabricated ohmic contacts in a satisfactory way.

Many (older) experiments investigating quantum Hall effects have simply used a cleaved square as a sample, without any further processing, and ohmic contacts are made by soldering In onto sample in several places around the perimeter, sometimes followed by a 425 °C anneal, but often without further annealing. Still the most popular metallization for an ohmic contact is composed of Ni, Au and Ge. (Ge is column IV, just below Si). After deposition, the contact is alloyed/thermally annealed by heating up the sample to typically ~ 400 °C for a few minutes (in order to minimize heating damage, some people use a rapid thermal annealer, where pre-heating and cooling occurs quickly). The metal elements have been seen to mix with the Ga and As in a complicated way, see Figure 2.7 and form new compounds in the process. Sometimes, it appears that spikes of highly doped material are protruding into the $GaAs$, and that the current mainly transfers through these spikes, as illustrated in Figure 2.12. It is thought that the Ni, which wets $GaAs$ very well, acts to prevent "balling up" of the $AuGe$. Variants exist that use nonmagnetic Pt instead of Ni.
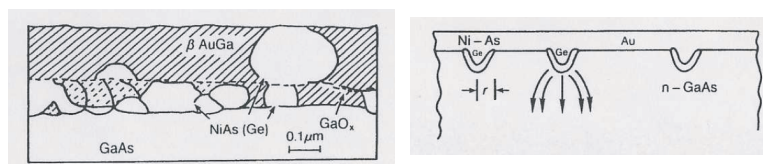

Figure 2.12: left: Various metal phases are present after annealing a $NiAuGe$ contact at 440 °440 for 2 min. right: A model for ohmic contacts in which conduction takes place trough a parallel array of Ge-rich protrusions [Look 1988]

2.8   Schottky gates

When quantum dots and other nanostructures formed in a 2DEG are defined using lateral metal gates (often $TiAu$ or $CrAu$ on the $GaAs$ surface (Ti and Cr act as adhesion layers)), one commonly applies sufficiently negative voltages to deplete electrons underneath gates. Controlling the voltage on the gate controls size of the depletion region and therefore the confinement potential of the device *in situ*. Since this is done in reverse bias of the Schottky diode, the currents flowing through the gates are exceedingly small, which is very important. Appreciable currents flowing from gates (i.e. gate leakage) can completely obliterate the small currents that one would like to measure through the device (in absence of gate leakage), and can also cause heating, decoherence, noise and other undesired effects. This is occasionally an issue due to various problems, but usually, metals make excellent Schottky barriers on the $GaAs$ surfaces or 2DEG materials. $GaAs$ is said to be *gateable*.

Mesa

Gate pad

Ohmic contact

1 mm

100 µm

1 µm   3.00kV

25 µm

5 µm   3.00kV